Enhanced spontaneous emission from two-photon-pumped quantum dots in a porous silicon microcavity

DMITRIY DOVZHENKO,[1,2,*] VICTOR KRIVENKOV,[1] IRINA KRIUKOVA,[1,3] PAVEL SAMOKHVALOV,[1] ALEXANDER KARAULOV,[4] AND IGOR NABIEV[1,3,4,*]

[1]*National Research Nuclear University MEPhI (Moscow Engineering Physics Institute), 115409 Moscow, Russia*
[2]*Department of Physics and Astronomy, University of Southampton, Southampton, SO17 1BJ, United Kingdom*
[3]*Laboratoire de Recherche en Nanosciences, LRN-EA4682, Université de Reims Champagne-Ardenne, 51100 Reims, France*
[4]*Sechenov First Moscow State Medical University (Sechenov University), 119146 Moscow, Russia*
**Corresponding authors: dovzhenkods@gmail.com (DD) or igor.nabiev@univ-reims.fr (IN)*

Received XX Month XXXX; revised XX Month, XXXX; accepted XX Month XXXX; posted XX Month XXXX (Doc. ID XXXXX); published XX Month XXXX

Photoluminescence (PL)-based sensing techniques have been significantly developed in practice due to their key advantages in terms of sensitivity and versatility of the approach. Recently, various nanostructured and hybrid materials have been used to improve the PL quantum yield and spectral resolution. The near-infrared (NIR) fluorescence excitation has attracted much attention because it offers deep tissue penetration and avoiding the autofluorescence of the biological samples. In our study, we have shown both spectral and temporal PL modifications under two-photon excitation of quantum dots (QDs) placed in one-dimensional porous silicon photonic crystal (PhC) microcavities. We have demonstrated an up to 4.3-fold Purcell enhancement of the radiative relaxation rate under two-photon excitation. The data show that the use of porous silicon PhC microcavities operating in the weak coupling regime permits the enhancement of the PL quantum yield of QDs under two-photon excitation, thus extending the limits of their biosensing applications in the NIR region of optical spectrum. © 2020 Optical Society of America

Light–matter resonance interaction enables control over spontaneous photoluminescence (PL) emission properties of various luminophores, including organic dyes [1,2], rare-earth ions [3], 2D metal dichalcogenides [4], and fluorescent nanocrystals [5,6]. The so-called "weak" coupling regime makes it possible to change the spectral, spatial, and temporal properties of the luminophore PL emission by varying the local electro-magnetic environment [7]. The use of photonic crystals (PhCs) is one of the most promising approaches to controlling the electromagnetic field distribution and, hence, to coupling it to the emitters placed inside the PhC microcavities (MCs) [1,3,4,7]. This approach is of special interest in the field of sensing in such emerging areas as the healthcare, environmental monitoring, and food safety [8,9]. Recent studies have demonstrated significant advances of PL-based sensors employing PhC structures in order to improve the critical properties of PL labels [9,10]. Porous silicon (pSi) MCs have been shown to be promising for biosensing applications due to the simplicity and scalability of fabrication and highly developed pore structure making the sensor surface easily accessible for analytes [11–13]. However, the necessity of selective excitation of majority of conventional dyes in the visible region of optical spectrum, low photostability, brightness, and background due to the autofluorescence of biological samples remain the obstacles to wider use of PL-based biosensor techniques. Excitation of the PL probes in the near-infrared (NIR) transparency window of biological samples could resolve some of these problems, allowing one deeper tissue penetration, higher spectral resolution and avoiding the autofluorescence. The nonlinear regime of two-photon excitation is a way to obtain visible-range fluorescence using NIR light sources. Moreover, the use of semiconductor quantum dots (QDs) with uniquely high two-photon absorption cross-sections compared to conventional dyes [14,15] allows one to reach the unprecedentedly high values of fluorescence contrast [16]. In addition, QDs are the excellent probes for sensing due to their wide one- and two-photon absorption [17,18] and narrow PL spectra, high quantum yield [19], and excellent photostability [20,21].

In this study, we have investigated the spontaneous PL emission of CdSe(core)/ZnS/CdS/ZnS(multishell) QDs placed inside a porous silicon MCs under two-photon excitation. We have measured the spectral and temporal characteristics of the spontaneous PL emission of QDs under two-photon pumping, as well as their dependence on the pump power. Significant enhancement of the QD PL at the wavelength corresponding to the MC eigenmode and its suppression within the photonic bandgap were observed. The change in the QD PL spectrum inside the porous silicon microcavity depended on the excitation energy density because the relaxation rates of the PL signal in the spectral regions where it was enhanced or suppressed were different. The increase in the emission rate corresponding to the weak coupling

between the exciton transition of QDs and the eigenmode of the MC has been shown, and Purcell factor was determined to be about 4.3.

Porous silicon microcavities were fabricated using the standard electro-chemical etching technique described elsewhere [22,23]. A pSi Fabry-Perot MC consisted of two Bragg mirrors with 5 and 20 pairs of porous layers with alternating high (75%) and low (58%) porosities separated with a high-porosity layer of double thickness forming a λ/2 cavity. After fabrication, pSi microcavities were thermally oxidized [24] in order to prevent QD PL from quenching due to the interaction with the silicon surface. In addition, the pSi surface was treated with hexadecyltrimethoxysilane in order to make it hydrophobic and improve the embedding of QDs from a solution. Fig. 1 shows the reflectance spectrum of the pSi MC (a) and scanning electron microscopy (SEM) images of its cross-section (b) and surface (c). It can be seen that the layers of high and low porosity form two distributed Bragg reflectors with a relatively homogeneous distribution of pores with diameters ranging approximately from 10 to 20 nm.

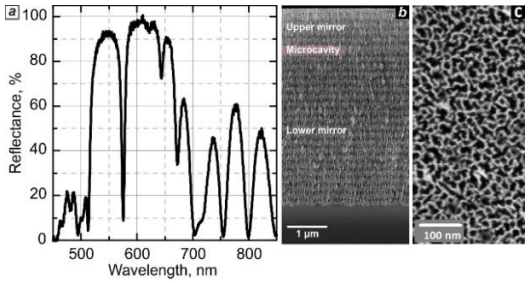

Fig. 1. The reflectance spectrum of the porous silicon microcavity (a) and scanning electron microscopy images of the cross-section (b) and the surface (c) of the fabricated porous silicon microcavity.

The photonic bandgap of the MC was approximately 154 nm wide (522–676 nm), with its eigenmode centered at 581 nm and a Q-factor of about 83. This MC design was chosen in order to provide partial matching between the QD emission maximum (Fig. 2) and the MC eigenmode, and to suppress the rest of the inhomogeneously broadened PL which remained uncoupled. By doing this, we were able to achieve enhancement of a significant part of the PL emission from the ensemble of QD placed in the MC.

CdSe(core)/ZnS/CdS/ZnS(multishell) QDs were fabricated using the hot injection method, as described elsewhere [25]. The absorption and PL spectra of a QD solution in hexane are shown in Fig. 2. QDs in a hexane solution had a wide absorption band with the first exciton peak about 536 nm. The PL spectrum of the QDs represents a symmetrical Gaussian curve with the maximum located at 560 nm and a full width at half maximum (FWHM) of about 40 nm.

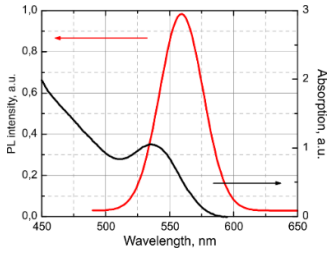

Fig. 2. The absorption (black line) and photoluminescence (PL, red line) spectra of CdSe(core)/ZnS/CdS/ZnS(multishell) QDs in a hexane.

Embedding of QDs into the pSi substrate was performed by drop-casting 5 μl of the hexane solution with a QD concentration of about 0.5 mg/ml onto the porous surface. Previously we have demonstrated that the treatment of the pSi surface described above, along with the proper design of the porous PhC morphology ensuring strong capillary forces [1], lead to a homogeneous distribution of QDs inside the pSi MC [26]. For PL measurements under two-photon-excitation, we have used a Tsunami femtosecond laser system (Spectra Physics, USA) with a pulse duration of 60 fs, tuneable pulse energy, and repetition rate of 80 MHz, operating at a wavelength of 800 nm. The laser beam divergence was about 10^{-3}. The measurements were performed in the confocal geometry, in which the laser beam was focused on the sample with a lens (with a focal length 30 mm); the same lens was used to collect the PL signal. The collected signal was spectrally resolved and recorded by the M266 monochromator-spectrograph (Solar Laser Systems, Belarus). The time-resolved measurements were performed using a time-correlated single photon counting system based on a Pico Harp 300 electronic module (PicoQuant) and a single photon avalanche diode from Micro Photon Devices (the final instrument response function of the system was 200 ps).

Fig. 3 shows the PL spectra of QDs placed inside the pSi MC under two-photon excitation at various values of the pumping laser power. Importantly, no difference of the PL spectra of QDs was observed under the single-photon and two-photon excitation regimes.

One can see that after embedding of the QDs into the pSi MC, their PL spectra split into two peaks (Fig. 3a). The first one at 575 nm with an FWHM of about 15 nm precisely corresponds to the wavelength of the MC eigenmode and may be related with the effect of weak coupling of QDs with the MC eigenmode reported previously [5,22]. The second peak at 550 nm has the same FWHM as the QDs in the solution (about 40 nm) and can be attributed to the uncoupled part of the QD ensemble, whose emission was partially suppressed inside the photonic bandgap due to the lowered local density of the optical states.

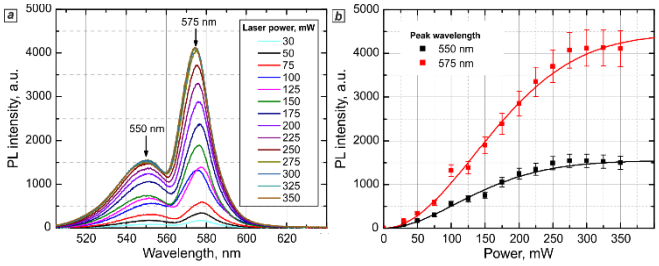

Fig. 3. Two-photon-excited photoluminescence (PL) spectra of the CdSe(core)/ZnS/CdS/ZnS(multishell) quantum dots (QDs) inside the porous silicon microcavity. (a) PL spectra of the QDs inside the microcavity under two-photon excitation at various laser pump powers. (b) The corresponding PL intensity dependences on the pump power at 575 nm (red) and 550 nm (black).

Otherwise, the PL maximum of uncoupled QDs is shifted by 10 nm towards the blue region relative to the maximum of the QD PL spectrum in the solution. It should be noted that homogeneous and inhomogeneous broadenings almost equally contribute to the overall broadening of the QD PL spectrum [27]. However, only the QDs whose homogeneously broadened PL spectra overlap with the MC eigenmode can be effectively coupled to it [7]. The QD PL maximum was initially shifted by 15 nm towards the blue region relative to the MC eigenmode. Therefore, the mixed nature of spectral broadening and spectral shift led to splitting of the QD ensemble into two parts after embedding into the pSi MC. The first part was effectively coupled to the

MC eigenmode, which resulted in a narrower PL peak at the MC eigenmode wavelength, while the second one, with PL shifted towards the blue region, fell into the pSi photonic bandgap and was subsequently suppressed.

In Fig. 3b, we have plotted the dependences of the PL peak intensities on the pump power in order to indirectly demonstrate that the two PL peaks have different radiative relaxation rates. As we increased the pump power, the initially quadratic dependence first turned into a near-linear one and then to a constant, indicating the saturation of two-photon absorption. However, the saturation threshold, estimated as the inflection point of the curves in Fig. 3b, was about 25% higher in the pump power for the 575 nm peak than for the 550 nm peak. It has been shown recently that under laser excitation with a high repetition rate (80 MHz in our case) the increase in the PL lifetime strongly shortens the absorption saturation threshold [17]. We approximated the experimental dependences with the equation from Ref. [17] (solid lines in Fig. 3b), assuming that the only possible difference between the parameters affecting the saturation threshold was the PL lifetime, whereas the two-photon absorption cross-sections were the same for QDs representing both peaks. If this is the case, then the observed difference in the saturation threshold can be only a result of the significant change in the radiative lifetime. Thus, if the PL lifetime of the 550 nm peak is equal to, or higher than, the repetition period (12.5 ns) of the excitation, the PL lifetime of the 575 nm peak should be much shorter than this period. Unfortunately, we could not precisely measure the rates of radiative relaxation for these peaks using our experimental setup, but our results indicate that the PL lifetime of the 575 nm peak is much shorter than that of the 550 nm peak, what is the signature of the Purcell effect.

Quantitative estimation of the Purcell factor could be made by comparing the radiative relaxation times extracted from the PL kinetics of the QDs coupled to the MC eigenmode and the uncoupled QD ensemble. In order to exclude the influence of the nonradiative relaxation pathways arising from the interaction of QDs with the surface of pSi, the control experiment has been made. We have compared the temporal properties of the PL of the QDs embedded inside the pSi MC at a wavelength of 575 nm with their properties in two control systems: (1) the QDs embedded inside the pSi monolayer with a fixed porosity of about 66%, which had the same thickness and the same degree of oxidation as the MC, and (2) the QDs dispersed in the poly(methyl methacrylate) (PMMA) matrix on a glass substrate. All PL kinetics were measured under two-photon excitation. The corresponding decay curves are shown in Figure 4. The total relaxation times of QD PL in the pSi MC and monolayer were calculated using amplitude weighting [28]. The results of the biexponential fit are presented in Table 1.

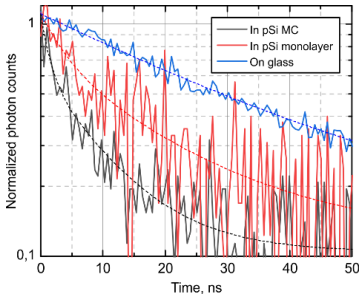

Fig. 4. The experimental (solid lines) and fitted (dashed lines) two-photon-excited PL decay of the QDs embedded in the porous silicon microcavity (black), embedded in the monolayer (red), and deposited onto a glass substrate (blue).

Table 1. Parameters of Biexponential Fitting of the PL Decay Curves for QDs Placed in the pSi Microcavities and in the Control Systems

QDs	A_1	τ_1, ns	A_2	τ_2, ns	τ_{AVG}, ns
in pSi MC	0.48	1.3	0.52	9.4	5.5
in pSi monolayer	0.4	3.73	0.60	18.0	12.3
in PMMA matrix on a glass substrate	1	30	-	-	30

It can be seen from Fig. 4 and Table 1 that the PL decay times for QDs in both the pSi MC and the monolayer were lower than for the QD film on the glass substrate. The experimental curve corresponding to the film of QDs in the PMMA matrix on the glass substrate could be well approximated by a monoexponential function with a decay time of about 30 ns, which was approximately the same as for the QDs in solution. The PL decay curves of QDs in both the pSi MC and the pSi monolayer were approximated by a biexponential function that had approximately equal contributions from the fast (1 to 4 ns) and slow (9 to 18 ns) decay components. Porous silicon is well known for its highly developed surface (up to 800 m^2/cm^3) [22]. As a result, significant part of embedded QDs was in a close vicinity to the pSi surface, which led to the appearance of non-radiative relaxation pathways for the embedded luminophores and, hence, decreased the total PL decay time. In experiments with both pSi substrates, the fast and slow decay components could be attributed to the QDs located directly on the surface of the pores and within them, respectively. The ratio between the average decay times of QDs in the pSi MC and pSi monolayer was about 2.2. The lack of additional non-radiative relaxation pathways in the case of the QD–PMMA film on glass compared to the QDs in the solution allowed us to estimate the Purcell factor, which is equal to the ratio between the radiative decay rates. For this purpose, we used the standard equation describing the value of PL quantum yield (QY):

$$QY = {\Gamma_r}/{(\Gamma_r + \sum \Gamma_{nr})}, \quad (1)$$

where Γ_r is the radiative relaxation rate and $\sum \Gamma_{nr}$ is the summary rate of all non-radiative relaxation processes. The PL quantum yield (QY) of QDs in solution was measured to be about 90%, while their decay kinetics was the same as for QDs embedded in the PMMA matrix on the glass substrate, with a decay time of 30 ns. The denominator in Eq. (1) is equal to one divided by the observed PL lifetime. Thus, Γ_r was estimated to be about 0.03 ns^{-1} outside of the pSi. As it was noted above, non-radiative relaxation pathways arose upon embedding of QDs into the pSi substrates due to the interaction of the former with the silicon surface. The overall non-radiative rate of relaxation in the pSi monolayer according to Eq. (1) was estimated to be about 0.052 ns^{-1}, which could be interpreted as a decrease in the QY down to 37%. Finally, presuming the same influence of non-radiative relaxation on the emission, we were able to estimate the Purcell enhancement factor of the radiative relaxation rate in the MC to be 4.3. The enhancement of the radiative relaxation rate of QD PL in the pSi MC of up to 0.130 ns^{-1} led to an increase in the QY of the QD ensemble to 71%.

In conclusion, we have investigated the spectral and temporal characteristics of spontaneous PL emission under two-photon excitation for QDs whose energy transitions are weakly coupled to the eigenmode of one-dimensional pSi MCs. An enhancement of the QD PL intensity was accompanied by a 4.3-fold increase in the radiative emission rate which is a signature for the occurrence of the Purcell effect. Finally, we have investigated the dependence of the emission spectra on the power of two-photon excitation and revealed a significant change in the PL spectra due to the difference between the relaxation rates of the enhanced and suppressed branches of PL. We have not observed any threshold or spectral narrowing in the dependence of the enhanced emission on the pump power density.

Two-photon-excited QD-based labels represent the promising platform for biosensing in the NIR region of optical spectrum, due to their much higher two-photon-absorption cross-sections compared to conventional dyes. However, the decrease in their PL QY due to nonspecific interaction with the surrounding media limits their brightness efficiency. Here, we have developed an approach to significantly increase the PL QY of QD under two-photon excitation by integrating the nanocrystals within the pSi photonic crystals. The data show that the use of pSi PhC microcavities operating in the weak coupling regime permit the enhancement of the PL quantum yield of QDs under two-photon excitation, thus extending the limits of their use in PL-based sensing, specifically, in the near-infrared spectral "transparency windows" of biological samples.

Acknowledgments. Support of Russian Foundation for Basic Research (RFBR), grant no. 18-29-20121, is acknowledged. I.N. thanks the Ministry of Higher Education, Research and Innovation of France and Region Grand Est of France for support. We thank the Department of Micro- and Nanosystems Physics (MEPHI) for the use of equipment and Vladimir Ushakov for the help with preparation of the manuscript.

Disclosures. The authors declare no conflict of interests.

References

1. N. A. Tokranova, S. W. Novak, J. Castracane, and I. A. Levitsky, "Deep infiltration of emissive polymers into mesoporous silicon microcavities: nanoscale confinement and advanced vapor sensing," J. Phys. Chem. C **117**, 22667–22676 (2013).
2. D. Dovzhenko, K. Mochalov, I. Vaskan, I. Kryukova, Y. Rakovich, and I. Nabiev, "Polariton-assisted splitting of broadband emission spectra of strongly coupled organic dye excitons in tunable optical microcavity," Opt. Express **27**, 4077 (2019).
3. S. N. A. Jenie, S. Pace, B. Sciacca, R. D. Brooks, S. E. Plush, and N. H. Voelcker, "Lanthanide luminescence enhancements in porous silicon resonant microcavities," ACS Appl. Mater. Interfaces **6**, 12012–12021 (2014).
4. X. Gan, Y. Gao, K. Fai Mak, X. Yao, R.-J. Shiue, A. van der Zande, M. E. Trusheim, F. Hatami, T. F. Heinz, J. Hone, and D. Englund, "Controlling the spontaneous emission rate of monolayer MoS2 in a photonic crystal nanocavity," Appl. Phys. Lett. **103**, 181119 (2013).
5. H. Qiao, B. Guan, T. Böcking, M. Gal, J. J. Gooding, and P. J. Reece, "Optical properties of II-VI colloidal quantum dot doped porous silicon microcavities," Appl. Phys. Lett. **96**, 161106 (2010).
6. C. Becker, S. Burger, C. Barth, P. Manley, K. Jäger, D. Eisenhauer, G. Köppel, P. Chabera, J. Chen, K. Zheng, and T. Pullerits, "Nanophotonic-enhanced two-photon-excited photoluminescence of perovskite quantum dots," ACS Photonics **5**, 4668–4676 (2018).
7. M. Pelton, "Modified spontaneous emission in nanophotonic structures," Nat. Photonics **9**, 427–435 (2015).
8. S. Arshavsky-Graham, N. Massad-Ivanir, E. Segal, and S. Weiss, "Porous silicon-based photonic biosensors: current status and emerging applications," Anal. Chem. **91**, 441–467 (2019).
9. C. Fenzl, T. Hirsch, and O. S. Wolfbeis, "Photonic crystals for chemical sensing and biosensing," Angew. Chemie Int. Ed. **53**, 3318–3335 (2014).
10. D. Threm, Y. Nazirizadeh, and M. Gerken, "Photonic crystal biosensors towards on-chip integration," J. Biophotonics **5**, 601–616 (2012).
11. C. Pacholski, "Photonic crystal sensors based on porous silicon," Sensors **13**, 4694–4713 (2013).
12. S. N. A. Jenie, S. E. Plush, and N. H. Voelcker, "Recent advances on luminescent enhancement-based porous silicon biosensors," Pharm. Res. **33**, 2314–2336 (2016).
13. M. B. de la Mora, M. Ocampo, R. Doti, J. E., and J. Faubert, "Porous silicon biosensors," in State of the Art in Biosensors - General Aspects (InTech, 2013), p. 141.
14. V. Krivenkov, P. Samokhvalov, D. Solovyeva, R. Bilan, A. Chistyakov, and I. Nabiev, "Two-photon-induced Förster resonance energy transfer in a hybrid material engineered from quantum dots and bacteriorhodopsin," Opt. Lett. **40**, 1440 (2015).
15. V. Krivenkov, P. Samokhvalov, and I. Nabiev, "Remarkably enhanced photoelectrical efficiency of bacteriorhodopsin in quantum dot – Purple membrane complexes under two-photon excitation," Biosens. Bioelectron. **137**, 117–122 (2019).
16. H. Hafian, A. Sukhanova, M. Turini, P. Chames, D. Baty, M. Pluot, J. H. M. Cohen, I. Nabiev, and J.-M. Millot, "Multiphoton imaging of tumor biomarkers with conjugates of single-domain antibodies and quantum dots," Nanomedicine Nanotechnology, Biol. Med. **10**, 1701–1709 (2014).
17. V. Krivenkov, P. Samokhvalov, D. Dyagileva, A. Karaulov, and I. Nabiev, "Determination of the single-exciton two-photon absorption cross sections of semiconductor nanocrystals through the measurement of saturation of their two-photon-excited photoluminescence," ACS Photonics **7**, 831–836 (2020).
18. R. Scott, A. W. Achtstein, A. Prudnikau, A. Antanovich, S. Christodoulou, I. Moreels, M. Artemyev, and U. Woggon, "Two photon absorption in II–VI semiconductors: the influence of dimensionality and size," Nano Lett. **15**, 4985–4992 (2015).
19. P. Linkov, P. Samokhvalov, K. Vokhmintsev, M. Zvaigzne, V. A. Krivenkov, and I. Nabiev, "Optical properties of quantum dots with a core–multishell structure," JETP Lett. **109**, 112–115 (2019).
20. V. Krivenkov, P. Samokhvalov, M. Zvaigzne, I. Martynov, A. Chistyakov, and I. Nabiev, "Ligand-mediated photobrightening and photodarkening of CdSe/ZnS quantum dot ensembles," J. Phys. Chem. C **122**, 15761–15771 (2018).
21. W. G. J. H. M. van Sark, P. L. T. M. Frederix, A. A. Bol, H. C. Gerritsen, and A. Meijerink, "Blueing, bleaching, and blinking of single CdSe/ZnS quantum dots," ChemPhysChem **3**, 871–879 (2002).
22. M. J. Sailor, "Porous silicon in practice: preparation, characterization and applications," in Porous silicon in practice: preparation, characterization and applications (Wiley-VCH Verlag GmbH & Co. KGaA, 2011), p. 77.
23. D. Dovzhenko, I. Martynov, P. Samokhvalov, E. Osipov, M. Lednev, A. Chistyakov, A. Karaulov, and I. Nabiev, "Enhancement of spontaneous emission of semiconductor quantum dots inside one-dimensional porous silicon photonic crystals," Opt. Express **28**, 22705 (2020).
24. A. E. Pap, K. Kordás, G. Tóth, J. Levoska, A. Uusimäki, J. Vähäkangas, S. Leppävuori, and T. F. George, "Thermal oxidation of porous silicon: Study on structure," Appl. Phys. Lett. **86**, 041501 (2005).
25. P. Samokhvalov, P. Linkov, J. Michel, M. Molinari, and I. Nabiev, "Photoluminescence quantum yield of CdSe-ZnS/CdS/ZnS core-multishell quantum dots approaches 100% due to enhancement of charge carrier confinement," Proc. SPIE - Int. Soc. Opt. Eng. **8955**, 89550S (2014).
26. D. S. Dovzhenko, I. L. Martynov, P. S. Samokhvalov, K. E. Mochalov, A. A. Chistyakov, and I. Nabiev, "Modulation of quantum dot photoluminescence in porous silicon photonic crystals as a function of the depth of their penetration," Proc. SPIE - Int. Soc. Opt. Eng. **9885**, 988507 (2016).
27. B. Fisher, J. M. Caruge, D. Zehnder, and M. Bawendi, "Room-temperature ordered photon emission from multiexciton states in single CdSe core-shell nanocrystals," Phys. Rev. Lett. **94**, 087403 (2005).
28. J. R. Lakowicz, "Introduction to fluorescence," in Principles of Fluorescence Spectroscopy (Springer US, 2006), p. 141-142.